Angewandte Chemie
Eine Zeitschrift der Gesellschaft Deutscher Chemiker

Supporting Information

Structure of the Ribosomal RNA Decoding Site Containing a Selenium-Modified Responsive Fluorescent Ribonucleoside Probe

Ashok Nuthanakanti[+], Mark A. Boerneke[+], Thomas Hermann, and Seergazhi G. Srivatsan**

anie_201611700_sm_miscellaneous_information.pdf

Supporting Information

1. Materials: 5-iodouridine, selenophene, *n*-butyllithium, tributyltin chloride, *bis*(triphenylphosphine)-palladium(II) chloride, 4,4'-dimethoxytrityl chloride, paromomycin, tobramycin and hygromycin were obtained from Sigma-Aldrich. Neomycin was procured from Fluka. 2-cyanoethyl-*N*,*N*-diisopropylchlorophosphoramidite was purchased from Alfa Aesar. TBDMS-protected ribonucleoside phosphoramidite substrates and solid supports required for RNA synthesis were purchased from Glen Research. All other reagents for solid-phase oligonucleotide (ON) synthesis were obtained from ChemGenes Corporation. Custom synthesized RNA ONs were purchased from Dharmacon RNAi Technologies, deprotected according to the supplier's protocol, PAGE-purified and desalted using Sep-Pak Classic C18 cartridge. Chemicals (BioUltra grade) for preparing buffer solutions were purchased from Sigma-Aldrich. Autoclaved water was used for preparation of all buffer solutions and in biophysical analysis.

2. Instrumentation: NMR spectra were recorded on a 400 MHz Jeol ECS-400 spectrometer. Mass measurements were recorded on the Applied Biosystems 4800 Plus MALDI TOF/TOF

analyzer and Water Synapt G2 High Definition mass spectrometers. Modified RNA ONs were synthesized on Applied Biosystems RNA/DNA synthesizer (ABI-394). Absorption spectra were recorded on Shimadzu UV-2600 spectrophotometer. HPLC analysis was performed using Agilent Technologies 1260 Infinity. UV-thermal melting studies of ONs were performed on Cary 300Bio UV-Vis spectrophotometer and CD analysis was performed on JASCO J-815 CD spectrometer. Steady-state and time-resolved fluorescence experiments were carried out in a micro fluorescence cuvette (Hellma, path length 1.0 cm) on Horiba Jobin Yvon, Fluorolog-3. Crystal screening and X-ray diffraction data were collected at 110 K on a Rigaku rotating anode X-ray generator (λ = 1.54 Å) equipped with a MAR345 imaging plate detector system.

3. Synthesis of 5-selenophene-modified uridine phosphoramidite substrate 2

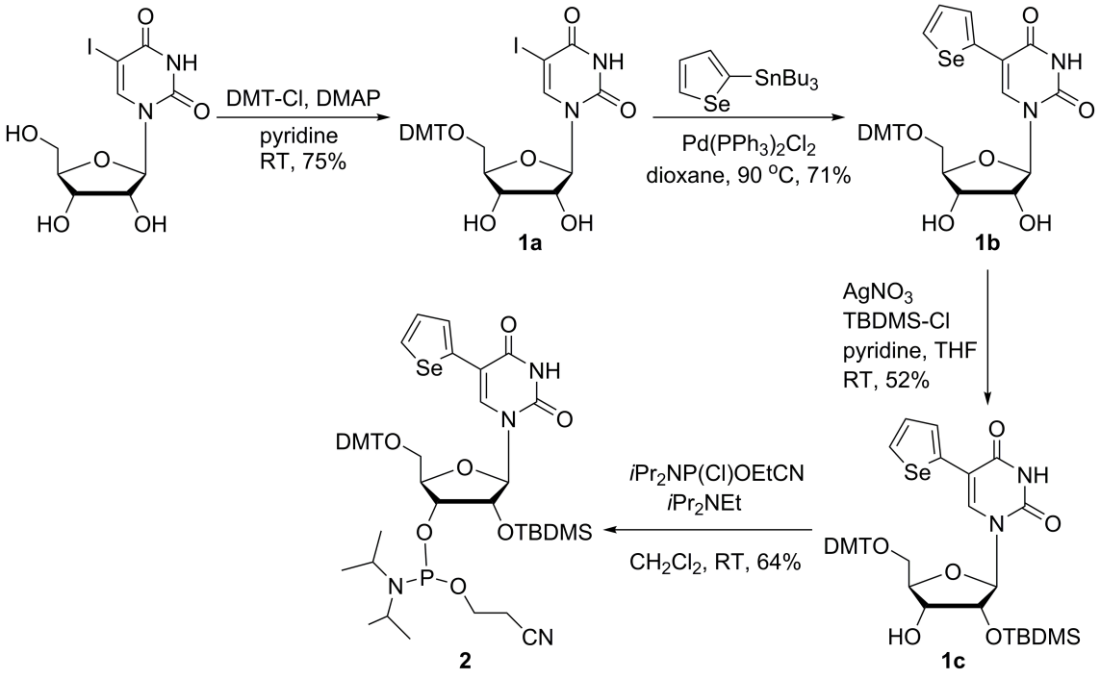

Scheme S1. Synthesis of 5-selenophene-modified uridine phosphoramidite substrate **2**.

5-Selenophene-modified 5'-*O*-DMT-protected uridine 1b: A mixture of 5'-*O*-DMT-protected 5-iodouridine **1a**[S1] (1.0 g, 1.49 mmol, 1.0 equiv), 2-(tri-*n*-butylstannyl)selenophene[S2] (1.37 g, 3.27 mmol, 2.2 equiv) and *bis*(triphenylphosphine)-palladium(II) chloride (0.084 g, 0.12 mmol, 0.08 equiv) was dissolved in anhydrous dioxane (25 ml). The reaction mixture was heated at 90 °C for 2 h and filtered through celite pad. The celite pad was washed with dichloromethane (2 × 20 ml), filtrate was evaporated and the resulting residue was purified by silica gel column chromatography to afford compound **1b** as an off white foam (0.71 g, 71% yield). TLC (CH_2Cl_2:MeOH = 95:5 with few drops of Et_3N); R_f = 0.36; ^{1}H NMR (400 MHz, $CDCl_3$): δ (ppm) 8.02 (s, 1H), 7.85 (dd, J_1 = 5.0 Hz, J_2 = 1.4 Hz, 1H), 7.40–7.38 (m, 2H), 7.28–7.26 (m, 4H), 7.23–7.15 (m, 3H), 6.85–6.83 (m, 2H), 6.77–6.75 (m, 4H), 5.99 (d, J = 4.8 Hz, 1H), 4.49 (t, J = 5.0 Hz, 1H), 4.35 (t, J = 4.6 Hz, 1H), 4.32–4.31 (m, 1H), 3.73 (s, 6H), 3.49–3.47 (m, 1H), 3.35 (dd, J_1 = 10.6 Hz, J_2 = 3.8 Hz, 1H);

^{13}C NMR (100 MHz, $CDCl_3$): δ (ppm) 162.2, 158.7, 151.0, 144.4, 136.3, 135.6, 135.5, 132.0, 130.1, 130.1, 128.9, 128.2, 128.1, 127.2, 124.7, 113.4, 112.2, 90.7, 86.9, 84.8, 75.6, 71.2, 63.4, 55.3; HRMS: m/z Calcd. for $C_{34}H_{33}N_2O_8Se$ $[M+H]^+$ = 677.1402, found = 677.1394.

5-Selenophene-modified 2'-*O*-TBDMS protected uridine 1c: Compound **1b** (0.95 g, 1.41 mmol, 1.0 equiv) and silver nitrate (0.62 g, 3.65 mmol, 2.6 equiv) were dissolved in anhydrous pyridine (4.8 ml). To the above solution was added anhydrous THF (14 ml). After stirring for 10 min *tert*-butyldimethylsilyl chloride (TBDMS-Cl, 0.55 g, 3.65 mmol, 2.6 equiv) was added. Reaction mixture was stirred for additional 0.5 h and filtered through celite pad. Celite pad was washed with ethyl acetate (2 × 15 ml) and the combined organic solution was then washed with 5 % sodium bicarbonate (20 ml) followed by brine solution (20 ml). The organic extract was dried over sodium sulphate and evaporated. The resulting crude residue was purified by silica gel column chromatography to afford the product **1c** as a white solid (0.57 g, 52% yield). TLC (petroleum ether:EtOAc = 60:40 with few drops of Et_3N); R_f = 0.42; ^{1}H NMR (400 MHz, $CDCl_3$): δ (ppm) 8.62 (br, 1H), 7.98 (s, 1H), 7.88 (d, J = 5.6 Hz, 1H), 7.42–7.40 (m, 2H), 7.30–7.28 (m, 5H), 7.24–7.19 (m, 2H), 6.78–6.67 (m, 6H), 6.12 (d, J = 5.6 Hz, 1H), 4.51 (t, J = 5.2 Hz, 1H), 4.26–4.22 (m, 2H), 3.74 (s, 6H), 3.54–3.52 (m, 1H), 3.40 (dd, J_1 = 11.0 Hz, J_2 = 3.0 Hz, 1H), 0.93–0.91 (s, 9H), 0.15 (s, 3H), 0.14 (s, 3H); ^{13}C NMR (100 MHz, $CDCl_3$): δ (ppm) 161.3, 158.8, 149.4, 144.4, 136.1, 135.4, 135.3, 132.6, 132.2, 130.2, 130.1, 128.9, 128.2, 128.1, 127.3, 124.9, 123.9, 113.4, 88.0, 87.0, 84.0, 75.8, 71.3, 63.4, 55.4, 25.8, 18.1, -4.5, -4.9; HRMS: m/z Calcd. for $C_{40}H_{46}N_2O_8SeSiNa$ $[M+Na]^+$ = 813.2086, found = 813.2123.

5-Selenophene-modified uridine phosphoramidite substrate 2: To a solution of compound **1c** (0.41 g, 0.52 mmol, 1.0 equiv) in anhydrous dichloromethane (4.1 ml) was added *N*,*N*-diisopropylethylamine (0.226 mL, 1.30 mmol, 2.5 equiv) and stirred for 10 min. To this solution was slowly added 2-cyanoethyl *N*,*N*-diisopropylchlorophosphoramidite (0.14 mL, 0.63 mmol, 1.2 equiv) and the reaction mixture was stirred for 12 h. The solvent was evaporated to dryness and the residue was redissolved in ethyl acetate (20 ml), which was washed with 5% sodium bicarbonate solution (15 ml) followed by brine solution (15 ml). The organic extract was dried over sodium sulphate, evaporated and the crude solid residue was purified by column chromatography to afford the product **2** as a white solid (0.33 g, 64%). TLC (petroleum ether:EtOAc = 60:40 with few drops of Et_3N); R_f = 0.40; Analytical data was obtained using one of the diastereomers, which eluted first. ^{1}H NMR (400 MHz, $CDCl_3$): δ (ppm) 8.03 (s, 1H), 7.86–7.84 (m, 1H), 7.44–7.42 (m, 2H), 7.32–7.28 (m, 5H), 7.25–7.20 (m, 2H), 6.78–6.70 (m, 6H), 6.12 (d, J = 6.4 Hz, 1H), 4.49 (t, J = 5.8 Hz, 1H), 4.37 (br, 1H), 4.24–4.20 (m, 1H), 3.74 (s, 6H), 3.61–3.51 (m, 5H), 3.30 (dd, J_1 = 10.6 Hz, J_2 = 2.6 Hz, 1H), 2.28–2.24 (m, 2H), 1.18–1.13 (m, 12H), 0.88 (s, 9H), 0.11 (s, 3H), 0.07 (s, 3H); ^{13}C NMR (100 MHz, $CDCl_3$): δ (ppm) 161.3, 158.8, 149.4, 144.4, 135.4, 132.8, 132.0, 130.3, 130.3, 130.2, 128.9, 128.4, 128.2, 128.1, 127.3, 124.8, 113.4, 87.6, 87.0, 84.2, 75.8, 74.9, 63.4, 55.4, 43.6, 43.5, 29.8, 25.8, 24.8, 22.7, 20.3, 18.1, -4.4, -4.7; ^{31}P NMR (162 MHz, $CDCl_3$): δ (ppm) 151.6; HRMS: m/z Calcd. for $C_{49}H_{63}N_4O_9PSeSiNa$ $[M+Na]^+$ = 1013.3165, found = 1013.3191.

4. Solid-phase synthesis of selenophene-modified RNA ON 3: RNA ON **3** was synthesized on a 1 μmole scale using CPG solid support (1000 Å). Standard synthesis cycles employed for 2'-*O*-TBDMS-protected phosphoramidite substrates was used. While incorporation of native 2'-*O*-TBDMS-protected phosphoramidites was performed with a coupling time of 10 min (two times), incorporation of 5-selenophene-modified-2'-*O*-TBDMS-protected

phosphoramidite substrate **2** was performed with a coupling time of 15 min (two times). The coupling efficiency for phosphoramidite substrate **2** based on trityl monitor-assay was found to be ~40%. After deprotection of trityl group on the synthesizer, the solid support was treated with a 1:1 solution of 10 M methylamine in ethanol and water (1.5 mL) for 12 h at RT. The mixture was centrifuged and the supernatant was evaporated to dryness on a Speed Vac. The residue was dissolved in DMSO (100 µL) and was added TEA.3HF (150 µL). The resulting solution was heated at 65 °C for 2.5 h and was brought to RT. The completely deprotected ON solution was lyophilized and was purified by PAGE (20% gel) under denaturing conditions. The band corresponding to the full-length product was identified by UV shadowing. The ON was extracted with ammonium acetate buffer (0.5 M, 3 ml) and desalted using a Sep-Pak classic C18 cartridge. A 1 µmol scale synthesis gave ~100 nmol of the labeled RNA after PAGE purification. See Figure S2 for HPLC chromatogram and mass spectrum of purified ON **3**. The selenophene-modified uridine was stable under solid-phase ON synthesis conditions. Standard deprotection and purification protocols (PAGA and HPCL) were used and the selenophene label was found to be stable and did not get oxidized. Under crystallization conditions also the modification was found to be stable (See section 9).

5. MALDI-TOF mass analysis of selenophene-modified RNA ON 3: 2 µL of the modified ON **3** (~200 µM) was combined with 1 µL of ammonium citrate buffer (100 mM, pH 9), 2 µL of a DNA internal standard (200 µM) and 4 µL of saturated 3-hydroxypicolinic acid solution. The sample was desalted using an ion-exchange resin (Dowex 50W-X8, 100-200 mesh, ammonium form), spotted on the MALDI plate and air dried.

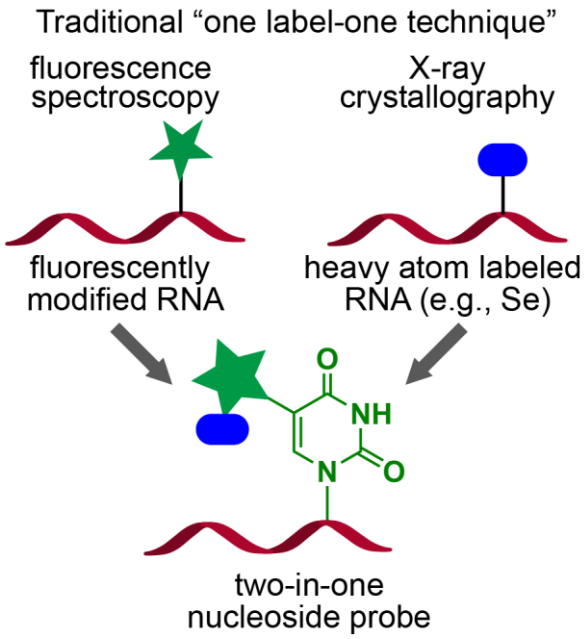

Figure S1. Design of "two-in-one" ribonucleoside probe for RNA analysis in solution and solid-state. In this design, the fluorophore core and anomalous X-ray scattering Se atom are placed in the same scaffold so that they sense the same environment when incorporated into RNA ONs.

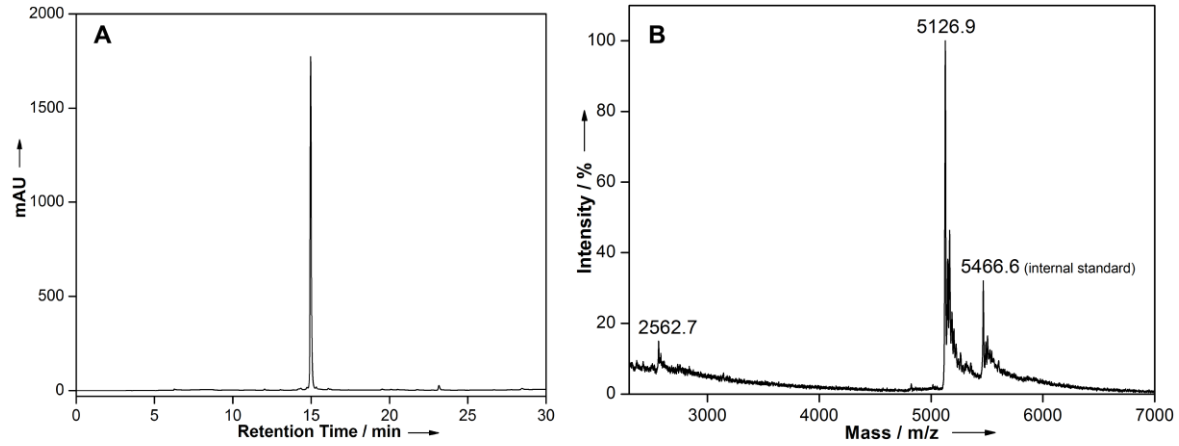

Figure S2. (**A**) HPLC chromatograms of PAGE purified ^{Se}U-modified ON **3** at 260 nm. Mobile phase A = 100 mM triethylammonium acetate buffer (pH 7.5), mobile phase B = acetonitrile. Flow rate = 1 mL/min. Gradient = 0–10% B in 10 min and 10–100% B in 20 min. HPLC analysis was performed using Luna C18 column (250 x 4.6 mm, 5 micron).
(**B**) MALDI-TOF mass spectrum of RNA ON **3**. The spectrum was calibrated relative to the +1 ion (m/z = 5466.6) of an internal DNA ON standard. Calcd. mass for ON **3**: $[M]^+$ 5127.1; found: $[M]^+$ 5126.9 and 2562.7 $[M]^{2+}$. For experimental details see section 5.

6. Reconstitution of bacterial A-site RNA models: A-site containing selenophene-modified uridine at position 1406 (**3•4**) and control native (**5•4**) A-site models were assembled by heating 1:1 mixture of respective ONs (40 µM) in buffer (30 mM sodium cacodylate, 100 mM NaCl, pH 6.8) at 70 °C for 3 min. Samples were slowly cooled to RT and placed on ice for 30 min before fluorescence, CD and thermal melting analysis were performed. For fluorescence and thermal melting analysis, samples of A-site constructs were diluted with cacodylate buffer to a final RNA concentration of 2 µM. For CD analysis, 5 µM concentration of A-site constructs was used.

7. CD analysis: 5 µM of the control unmodified and selenophene modified A-site constructs was used in the CD experiments. CD spectra were collected from 350 to 220 nm using a quartz cuvette (Sterna Scientific, path length 2 mm) on a Jasco J-815 CD spectrometer using 1 nm bandwidth at 20 °C. Experiments were performed in duplicate wherein each spectrum was an average of three scans. The spectrum of buffer was subtracted from all sample spectra.

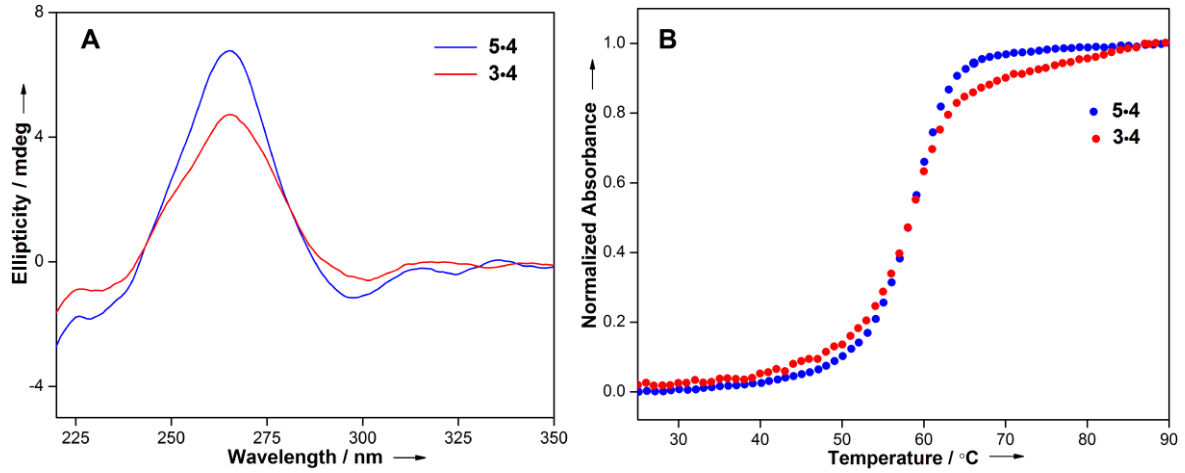

Figure S3. (**A**) CD spectra (5 μM) of control unmodified A-site RNA **5•4** (blue) and ^{Se}U-modified A-site RNA **3•4** (red). Both unmodified and modified ONs showed similar CD profiles, which were in consensus with the literature report.[S3] (**B**) UV-thermal melting profile of control A-site RNA **5•4** (blue) and ^{Se}U-modified A-site RNA **3•4** (red) at 260 nm. T_m values for **5•4** and **3•4** were found to be 59.0 ± 0.7 °C and 58.8 ± 0.3 °C, respectively. For experimental details see section 6 and 7.

8. Fluorescence monitoring of aminoglycosides binding to selenophene modified A-site construct 3•4: 400 μL of A-site construct **3•4** (2 μM) was taken in a micro fluorescence cuvette (Hellma, path length 1.0 cm) and titrated by adding 1 μL of stock solutions of increasing concentration of aminoglycosides. After each addition of aminoglycoside the sample was excited at 330 nm with excitation and emission slit widths of 4 and 6 nm, respectively, and changes in fluorescence intensity at emission maximum (450 nm) were measured. The aminoglycoside was added till the fluorescence saturation point. The total volume change upon addition of aminoglycosides throughout the titration was ≤ 4%. A spectral blank of cacodylate buffer in the absence of RNA and aminoglycoside was subtracted from all titrations. A control titration experiment performed as above by adding buffer (instead of aminoglycosides) to A-site **3•4** did not result in detectable changes in fluorescence indicating that repeated excitation of the sample did not cause photodegradation or photobleaching of the labeled A-site. Therefore, the increase in fluorescence intensity observed upon addition of aminoglycoside antibiotics to A-site reflects the ability of selenophene-modified uridine to report RNA-ligand binding. All fluorescence experiments were performed in triplicate at 20 °C. Normalized fluorescence intensity (F_N) versus log of aminoglycoside (AG) concentration plots were fitted using Hill equation (OriginPro 8.5.1) to determine the apparent dissociation constant (*KD*) values for the binding of aminoglycosides to A-site construct.[S4,S5] One-site binding model was used. χ^2 values for the curve fits were found to be very close to unity. Hill coefficient (n) was in the range of 1.2–1.5.

$$F_N = \frac{F_i - F_0}{F_s - F_0}$$

F_i is the fluorescence intensity at each titration point. F_0 and F_s are the fluorescence intensity in the absence of aminoglycoside and at saturation, respectively. n is the Hill coefficient or degree of cooperativity associated with the binding.

$$F_N = F_0 + (F_S - F_0)\left(\frac{[\mathrm{AG}]^n}{[KD]^n + [\mathrm{AG}]^n}\right)$$

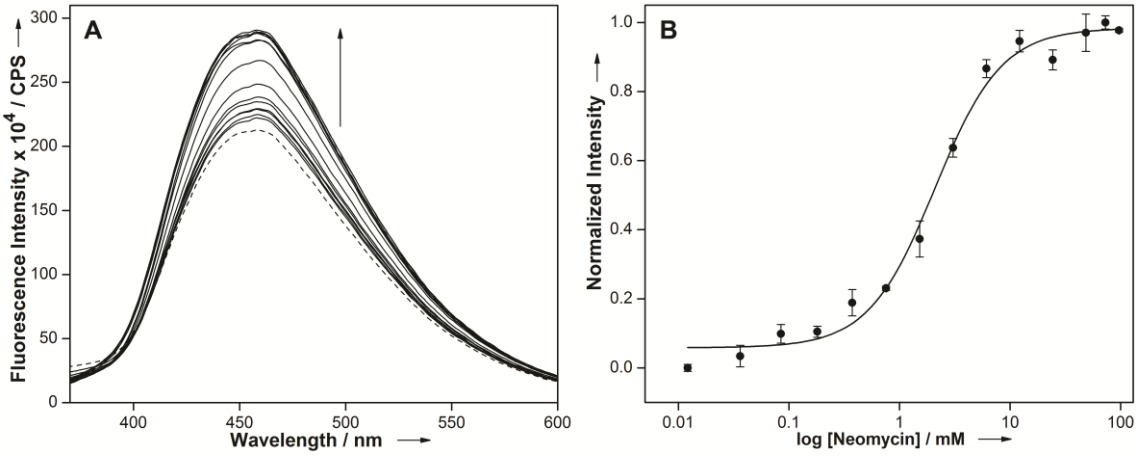

Figure S4. (**A**) Emission spectra (solid lines) of A-site **3•4** as a function of increasing concentration of neomycin B. Dashed line represents emission profile in the absence of aminoglycoside. (**B**) Curve fit for the titration of A-site with neomycin B. Normalized fluorescence intensity at λ_{em} = 450 nm is plotted against log [aminoglycoside].

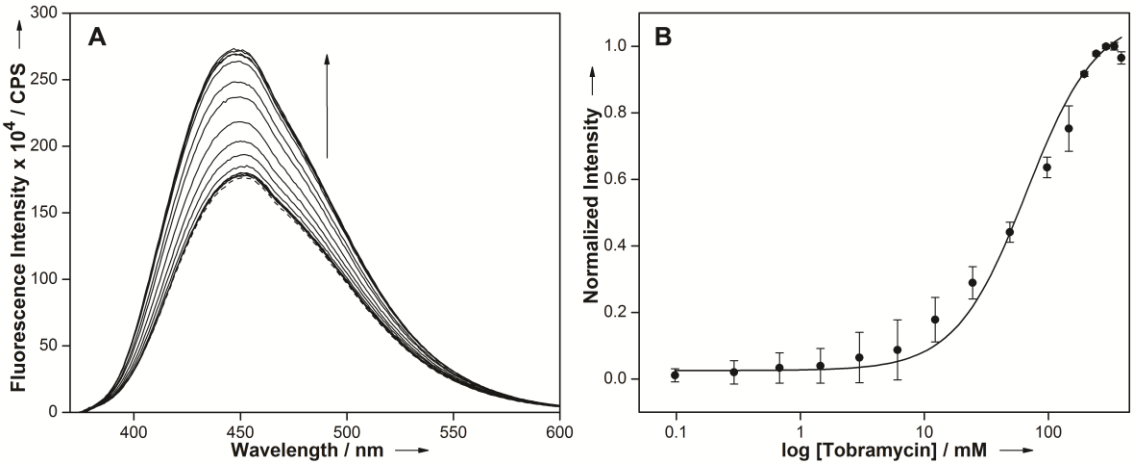

Figure S5. (**A**) Emission spectra (solid lines) of A-site **3•4** as a function of increasing concentration of tobramycin. Dashed line represents emission profile in the absence of aminoglycoside. (**B**) Curve fit for the titration of A-site with tobramycin. Normalized fluorescence intensity at λ_{em} = 450 nm is plotted against log [aminoglycoside].

9. Crystallization and Data Collection: The ^{Se}U-modified A-site model RNA **3•4** was assembled by annealing stoichiometric amounts of the ON **3** and **4** in 10 mM sodium cacodylate, pH 6.5 by heating to 65 °C for 4 min followed by snap cooling on ice for 10 min followed by slow warming to room temperature. After annealing, the RNA was crystallized at 22 °C by hanging drop vapor diffusion. For crystallization, 1 μL of 0.2 mM RNA was mixed with an equal volume of crystallizing solution containing 2.40–2.55 M ammonium sulfate, 10 mM magnesium acetate, and 40 mM 2-(*N*-morpholino)ethanesulfonic acid (MES) buffer (pH 5.6). Crystals grew over the course of four to seven months after equilibration against 700 μL of well solution containing crystallizing solution. Crystals were flash-cooled in liquid nitrogen. Crystal screening and X-ray diffraction data were collected at 110 K on a

Rigaku rotating anode X-ray generator (λ = 1.54 Å) equipped with a MAR345 imaging plate detector system. Datasets were processed, integrated, and scaled with the HKL2000 package.[S6]

Structure solution and refinement: The three-dimensional structures of the ^{Se}U-modified A-site RNA construct was solved by molecular replacement with the program Phaser[S7] using a previously determined structure,[S5] as the search model and refined by the program Refmac[S8] both within the CCP4 package.[S9] Subsequent iterative rounds of manual building and refinement, alternating between Refmac and manual rebuilding in Coot,[S10] were based on the obtained 2Fo-Fc and Fo-Fc density maps. Final refinement was carried out in PHENIX[S11] with individual isotropic atomic displacement parameters and water picking. Crystallographic data collection and refinement statistics are provided in Table S1. Atomic coordinates and structure factors of the ^{Se}U-modified A-site RNA have been deposited in the Research Collaboratory for Structural Bioinformatics (RCSB) Protein Data Bank, www.rcsb.org (PDB ID code 5T3K).

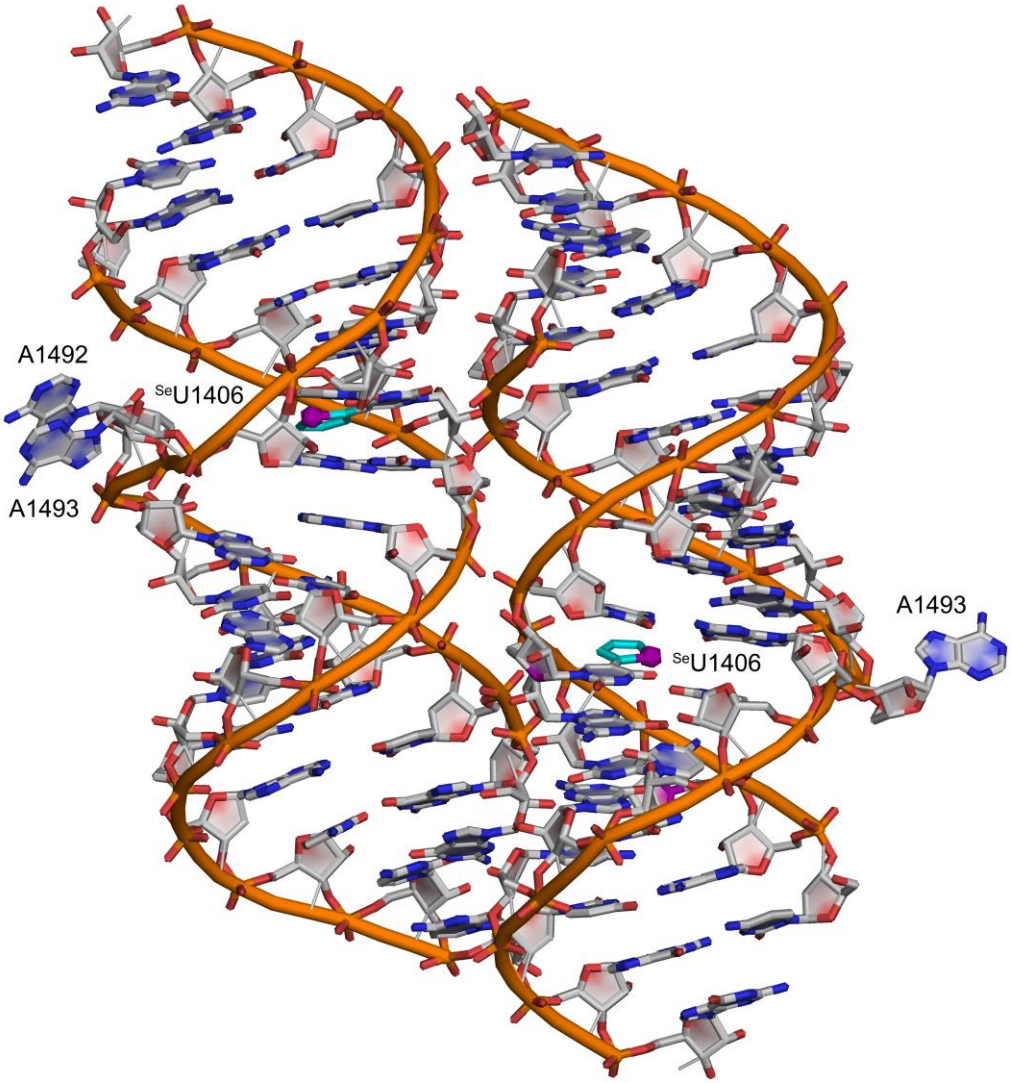

Figure S6. Crystal structure of ^{Se}U-modified A-site RNA **3•4** containing two unique A-sites with 50% occupancy in the unit cell. (left) RNA copy in which A1492 and A1493 residues are flipped-out of the loop. This structure closely resembles the structure of the decoding site bound to the aminoglycosides. (right) RNA copy in which only A1493 is flipped-out of the loop. SeU is shown in cyan color.

Table S1. Crystallographic data collection and refinement statistics.

Data Collection	
Wavelength (Å)	1.54
High-resolution limit (Å)	2.14
Low-resolution limit (Å)	26.02
Redundancy[a]	2.9 (1.7)
Completeness (%)[a]	77.6 (46.7)
$I/\sigma(I)$[a]	11.32 (4.25)
Total reflections	103258
Unique reflections	7483
Refinement	
Space group	$P2_1$
Cell dimensions (Å)	
a	31.55
b	86.96
c	32.56
α	90.00
β	94.14
γ	90.00
R_{work}/R_{free}	0.197 / 0.247
No. atoms	
RNA atoms	1408
Solvent atoms	60
Metal ions	10 Mg^{2+}
Mean *B* factors (Å^2)	
RNA	32.6
Solvent	32.2
Metal	37.5
R.m.s. deviations	
Bond lengths (Å)	0.007
Bond angles (°)	1.366
Dihedral angles (°)	20.892

[a]Numbers in parentheses are for the highest-resolution shell.

Table S2. Important H-bonding and stacking interactions present in control, ^{Se}U-modified A-site RNA constructs, and unmodified A-site RNA bound to aminoglycoside antibiotics.

A-site RNA construct	Hydrogen bond	distance (Å)	π-π distance (Å)[a]
Control A-site (PDB: 1T0D)			
G1405-C1496	N2H---O2	2.827	G1405 (Py)-U1406
	N1H---N3	2.857	3.769
	O6---HN	2.857	
U1406-U1495	N3H---O2	3.015	U1406-C1407
	O4---HN3	2.892	3.888
C1407-G1494	O2---HN2	2.741	
	N---HN1	2.791	
	NH---O6	2.818	
^{Se}U-modified **3•4** A-site (PDB: 5T3K)			
G1405-C1496	N2H---O2	2.588	G1405 (Py)-^{Se}U1406 (uracil)
	N1H---N3	2.857	3.701
	O6---HN	2.985	U1406-C1407
U1406-U1495	N3H---O2	3.166	3.713
	O4---HN3	2.913	G1405 (Im)-U1406 (Se)
C1407-G1494	O2---HN2	2.456	3.720
	N---HN1	2.716	
	NH---O6	2.823	
Paromomycin bound to A-site RNA (PDB: 1J7T)			
G1405-C1496	N2H---O2	2.206	G1405 (Py)-U1406
	N1H---N3	2.564	3.776
	O6---HN	2.776	U1406-C1407
U1406-U1495	N3H---O4	2.808	4.205
C1407-G1494	O2---HN2	2.429	
	N---HN1	2.873	
	NH---O6	3.220	
Neomycin bound to A-site RNA (PDB: 2A04)			
G1405-C1496	N2H---O2	2.530	G1405 (Py)-U1406
	N1H---N3	2.847	3.860
	O6---HN	3.035	U1406-C1407
U1406-U1495	O4---HN3	3.203	3.958
C1407-G1494	O2---HN2	2.891	
	N---HN1	2.892	
	NH---O6	2.767	
Tobramycin bound to A-site RNA (PDB: 1LC4)			
G1405-C1496	N2H---O2	2.711	G1405 (Py)-U1406
	N1H---N3	2.692	3.715
	O6---HN	2.564	U1406-C1407
U1406-U1495	N3H---O4	2.365	4.273
C1407-G1494	O2---HN2	2.444	
	N---HN1	2.577	
	NH---O6	2.583	

[a]Centroid to centroid distance has been reported.

Py = pyrimidine ring; Im = imidazole ring of guanine; Se = selenophene ring of ^{Se}U ribonucleoside.

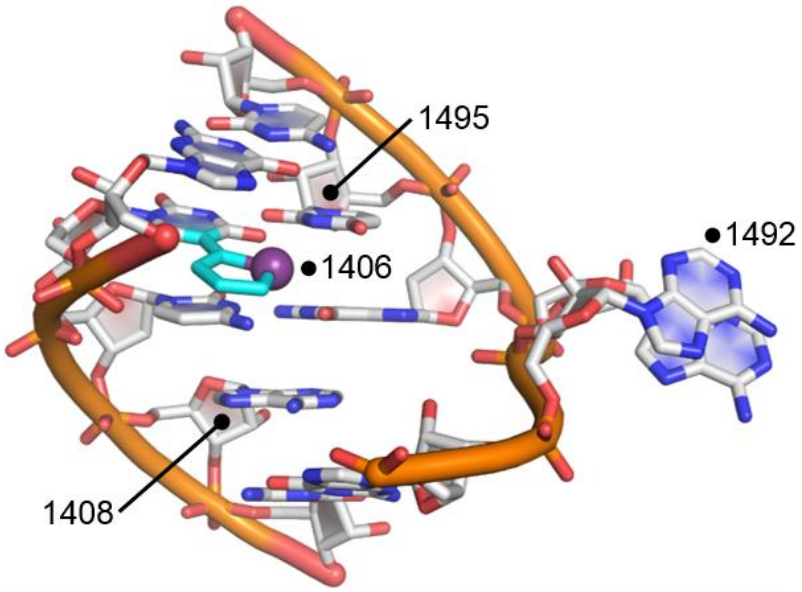

Figure S7. Structure showing noncanonical Watson-Crick pairing between ^{Se}U1406 and U1495 as in the native decoding site RNA.

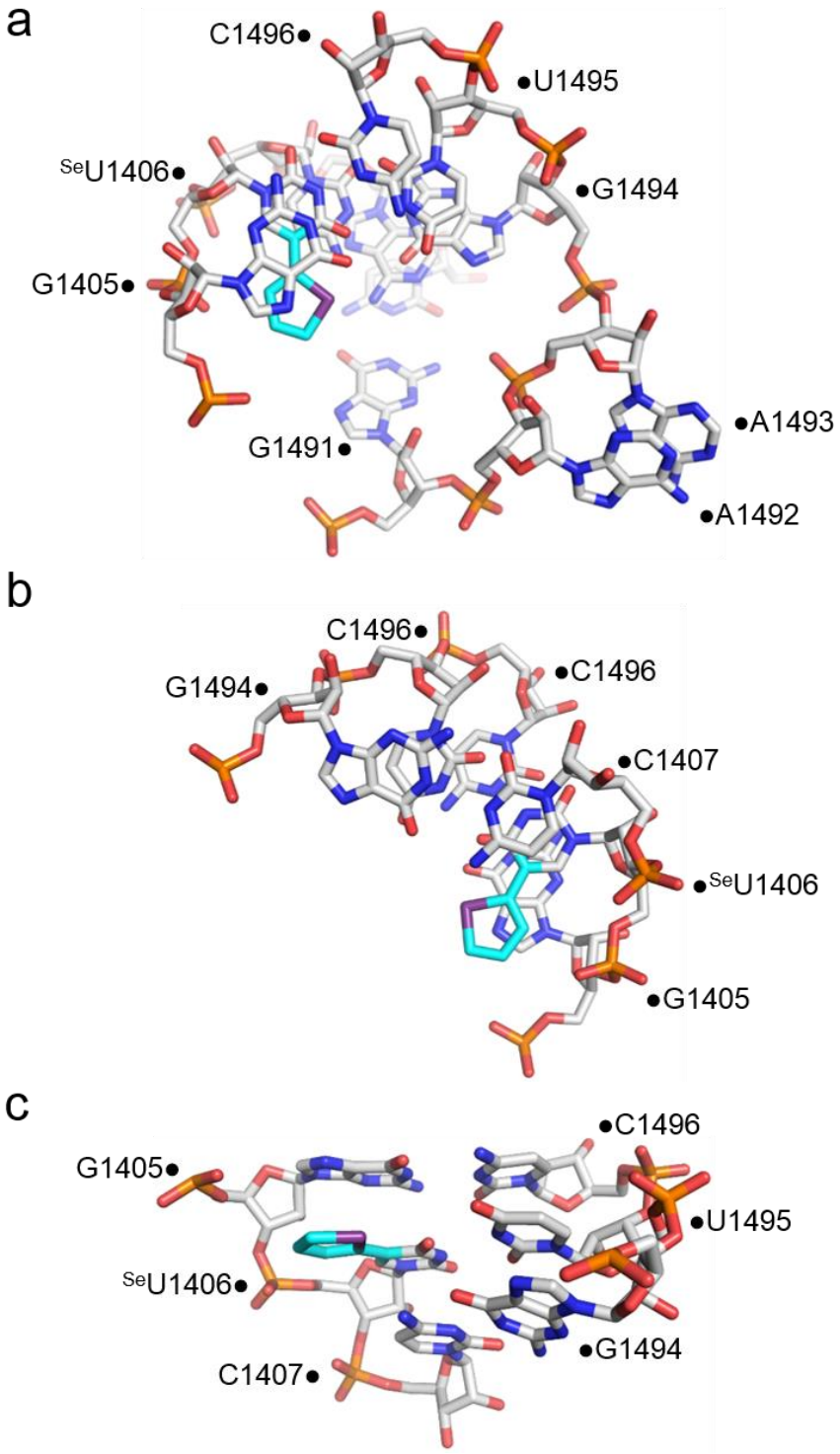

Figure S8. Stacking of ^{Se}U1406 with neighboring residues G1405 and C1407. (a) Top-down view with G1405 in the foreground in which the imidazole ring of G1405 is stacked with the selenophene ring of ^{Se}U. (b) Bottom-up view with C1407 in the foreground in which the uracil ring of ^{Se}U is stacked with the C1407 base. (c) Side view with G1405 above and C1407 below the ^{Se}U1406.

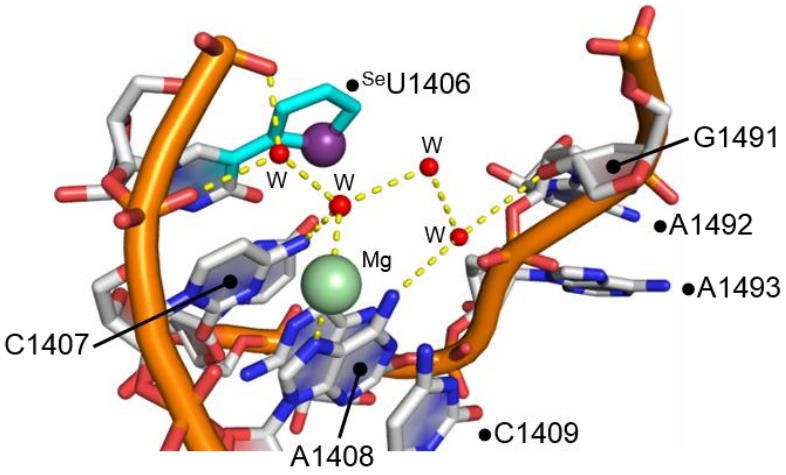

Figure S9. Structure showing the interaction between the 2'-OH group of G1491 and the N6 of A1408 through a bridging water molecule.

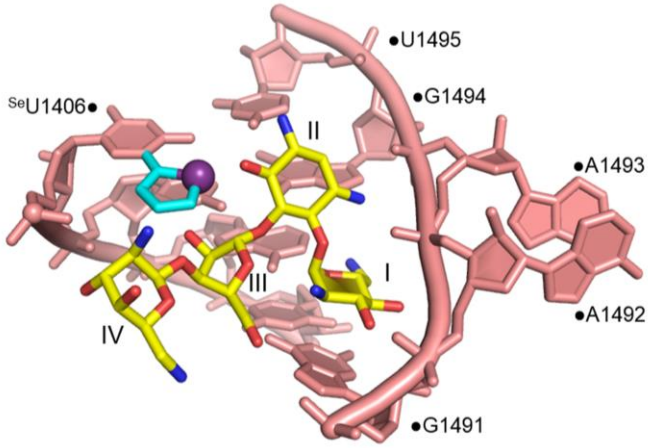

Figure S10. Superimposition of the ^{Se}U-modified A-site RNA and native A-site RNA bound to neomycin B (yellow; PDB: 2A04).[S25] Superimposed SeU nucleoside (cyan) is only shown.

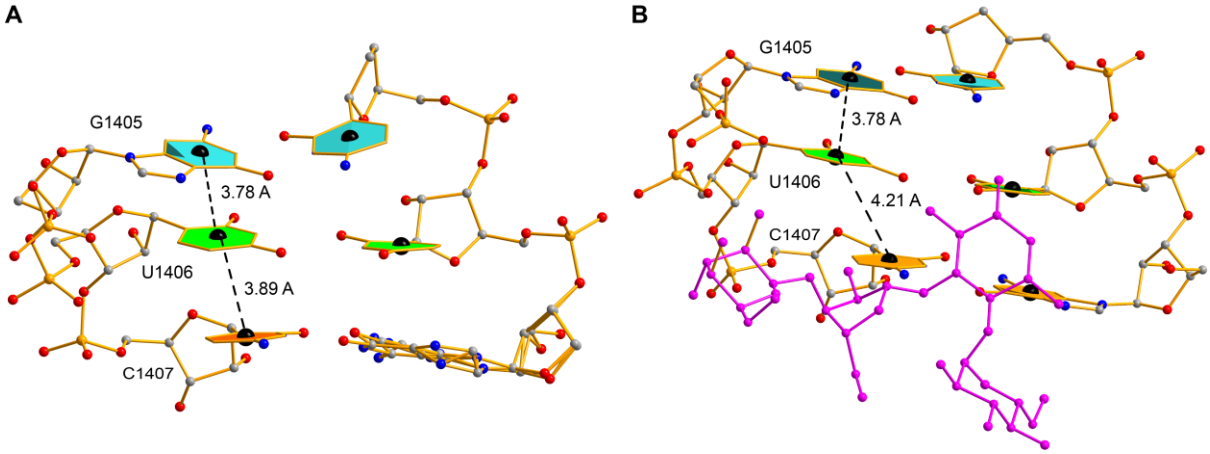

Figure S11. Comparison of stacking interactions between U1406 and its neighboring bases (G1405 and C1407) in the structure of the native A-site in the absence (**A**), and presence (**B**) of an aminoglycoside. A representative structure of aminoglycoside (paromomycin in magenta; PDB: 1J7T) bound to A-site RNA is shown here.

10. NMR Spectra

^{1}H NMR of the phosphoramidite of ^{Se}U **2** in $CDCl_3$ (400 MHz)

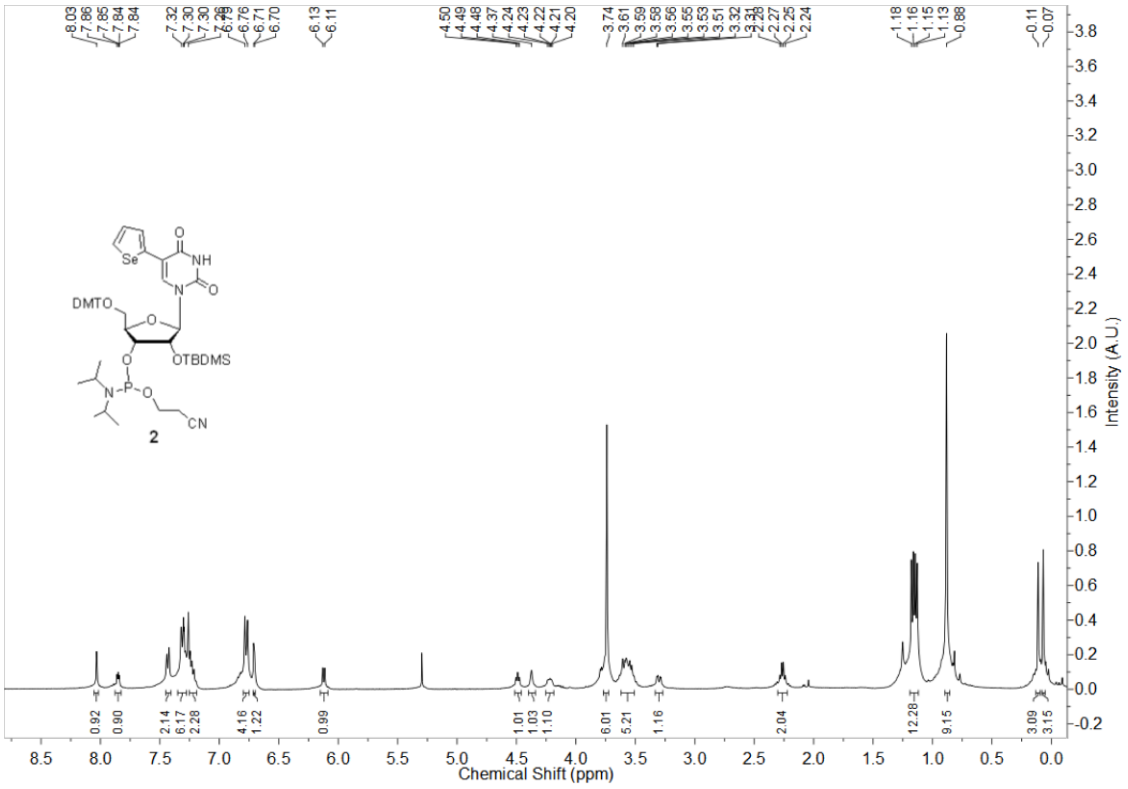

^{13}C NMR of the phosphoramidite of ^{Se}U **2** in $CDCl_3$ (100 MHz)

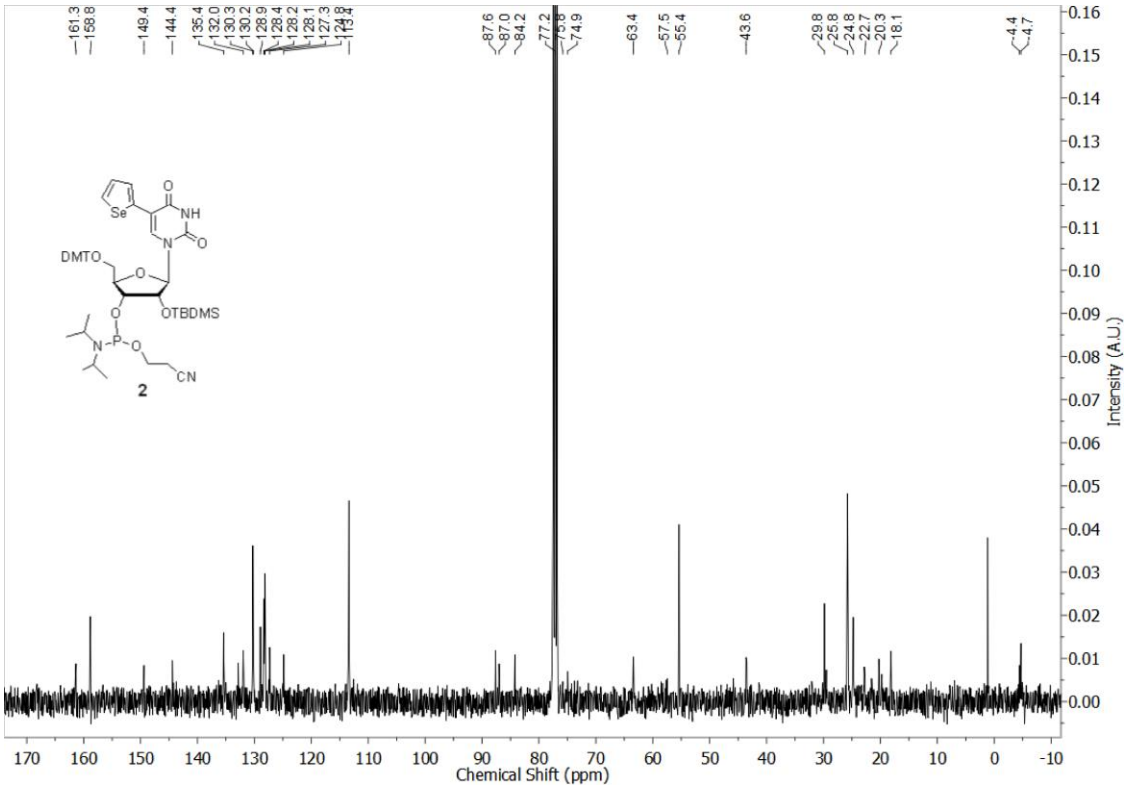

^{31}P NMR of the phosphoramidite of ^{Se}U **2** in $CDCl_3$ (162 MHz)

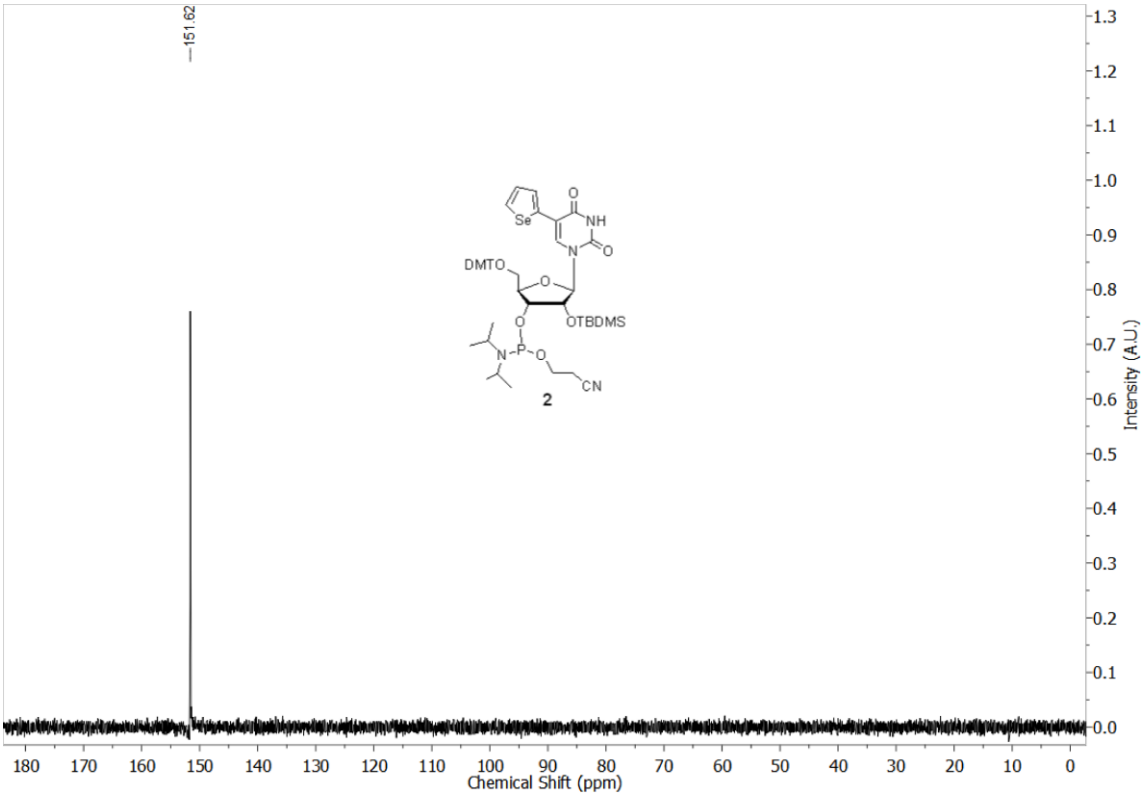

11. References

[S1] K. Shah, H. Wu, T. M. Rana, *Bioconjugate Chem.* **1994**, *5*, 508−512.

[S2] L. S. Liebeskind, J. Wang, *J. Org. Chem*. **1993**, *58*, 3550−3556.

[S3] C. M. Barbieri, M. Kaul, D. S. Pilch, *Tetrahedron* **2007**, *63*, 3567–3574.

[S4] a) V. K. Tam, D. Kwong, Y. Tor, *J. Am. Chem. Soc*. **2007**, *129*, 3257−3266; b) A. A. Tanpure, S. G. Srivatsan. *Nucleic Acids Res*. **2015**, *43*, e16.

[S5] S. Shandrick, Q. Zhao, Q. Han, B. K. Ayida, M. Takahashi, G. C. Winters, K. B. Simonsen, D. Vourloumis, T. Hermann, *Angew. Chem. Int. Ed*. **2004**, *43*, 3177–3182; *Angew. Chem*. **2004**, *116*, 3239–3244.

[S6] Z. Otwinowski, W. Minor, *Methods Enzymol.* **1997**, *276*, 307–326.

[S7] A. J. McCoy, R. W. Grosse-Kunstleve, P. D. Adams, M. D. Winn, L. C. Storoni, R. J. Read, *J. Appl. Crystallogr.* **2007**, *40*, 658–674.

[S8] G. N. Murshudov, A. A. Vagin, E. J. Dodson, *Acta Crystallogr., Sect D: Biol. Crystallogr.***1997**, *53*, 240–255.

[S9] *Acta Crystallogr., Sect D: Biol. Crystallogr.***1994**, *50*, 760–763

[S10] P. Emsley, K. Cowtan, *Acta Crystallogr., Sect D: Biol. Crystallogr*. **2004**, *60*, 2126–2132.

[S11] P. D. Adams, R. W. Grosse-Kunstleve, L.-W. Hung, T. R. Ioerger, A. J. McCoy, N. W. Moriarty, R. J. Read, J. C. Sacchettini, N. K. Sauter, T. C. Terwilliger, *Acta Crystallogr., Sect D: Biol. Crystallogr.* **2002**, *58*, 1948–1954.

[S12] F. Zhao, Q. Zhao, K. F. Blount, Q. Han, Y. Tor, T. Hermann, *Angew. Chem. Int. Ed*. **2005**, *44*, 5329−5334; *Angew. Chem*. **2005**, *117*, 5463−5468.

Complete author list for references 13b, 23 and 26 from the main article.

[13b] A. Serganov, S. Keiper, L. Malinina, V. Tereshko, E. Skripkin, C. Höbartner, A. Polonskaia, A. T. Phan, R. Wombacher, R. Micura, Z. Dauter, A. Jäschke, D. J. Patel, *Nat. Struct. Mol. Biol*. **2005**, *12*, 218–224.

[23] D. Perez-Fernandez1, D. Shcherbakov, T. Matt, N. C. Leong, I. Kudyba, S. Duscha, H. Boukari, R. Patak, S. R. Dubbaka, K. Lang, M. Meyer, R. Akbergenov, P. Freihofer, S. Vaddi, P. Thommes, V. Ramakrishnan, A. Vasella, E. C. Böttger, *Nat. Commun*. **2014**, *5*, 3112.

[26] J. R. Stagno, Y. Liu, Y. R. Bhandari, C. E. Conrad, S. Panja, M. Swain, L. Fan, G. Nelson,C. Li, D. R. Wendel, T. A. White, J. D. Coe, M. O. Wiedorn, J. Knoska, D. Oberthuer, R. A. Tuckey, P. Yu, M. Dyba, S. G. Tarasov, U. Weierstall, T. D. Grant, C. D. Schwieters, J. Zhang, A. R. Ferré-D'Amaré, P. Fromme, D. E. Draper, M. Liang, M. S. Hunter, S. Boutet, K. Tan, X. Zuo, X. Ji, A. Barty, N. A. Zatsepin, H. N. Chapman, J. C. H. Spence, S. A. Woodson and Y.-X. Wang, *Nature* **2017**, doi:10.1038/nature20599.